Turbulence and Flow Interplay in the Tokamak Edge Plasma

Ph. Ghendrih[1], P. Tamain[2], G. Chiavassa[3], G. Ciraolo[3], N. Fedorczak[1], X. Garbet[1], V. Grangirard[1], J. Gunn[1], P. Haldenwang[3], P. Hennequin[4], L. Isoardi[3], P. Monier-Garbet[1], C. Morize[4], Y. Sarazin[1], F. Schwander[1], E. Serre[3]

1) Association Euratom CEA, CEA/DSM/IRFM, Cadarache,
13108 Saint-Paul-lez-Durance, France,
2) present address: EURATOM/UKAEA Fusion Association, Culham Science Centre, Abingdon, Oxfordshire, OX14 3DB, UK
3) M2P2, UMR 6181, Ecole Centrale de Marseille, Technopole de Château Gombert,
38, Rue F. Joliot-Curie, 13451 Marseille Cedex 20, France
4) LPTP, UMR 7648 du CNRS, Ecole Polytechnique, 91128 Palaiseau, France

e-mail contact of main author: philippe.ghendrih@cea.fr

Abstract. The theoretical investigation of edge and SOL plasma turbulence indicates that the turbulence appears far less intermittent when the appropriate Log(N) field is used. Diffusive flow transport shows that the SOL parallel flow spreads into the core but exhibits a weak dependence on the Schmidt number. Conversely core flows strongly shifts the SOL stagnation point. The TOKAM-3D full torus transport and turbulence simulations allow one to recover the parallel flow pattern reported in the experiments, in particular with a Mach =0.4 from the low field side to the high field side at the top of the device.

1. Introduction

The interplay between large scale flows and turbulence is a matter of growing attention. This particular physics is observed to play a significant role in the transport properties that govern the edge operational scenarios in present devices as well as their projection to ITER [1]. Regarding core physics, the plasma rotation driven by turbulence can impact the MHD stability [1] as well as trigger the external H-mode barrier [1]. The generation of plasma rotation by turbulence is recognised as most important since the external torque is expected to be too small in next step devices such as ITER. Regarding the Scrape-Off Layer and divertor physics, large scale parallel flows have been reported for both limiter and divertor configurations [2, 3, 4]. These flows are particularly large when the so-called ion grad-B drift is oriented towards the X point in the divertor configuration or towards the limiter as on Tore Supra. They appear to be governed by the particle sources, in particular by the ballooned particle outflux from the core plasma [2]. In turn, they are expected to govern material migration from the low field side to the high field side. The propagation of such a flow pattern from the SOL into the edge plasma via turbulent momentum transport is regarded as one possible player in the onset of the H-mode transport barrier in the framework of turbulent eddies shearing by flows.

The theoretical investigation of these effects is quite challenging and requires a simulation effort to address the non-linear processes that take part in the interplay between turbulence and flows. The present work is based on a series of 3 fluid codes used to address specific properties of the interplay between turbulence and flows. The three main sections of the paper are organised accordingly. Section 2 is dedicated to SOL turbulence governed by the interchange instability [5]. The 2D turbulence code TOKAM-2D [5] is used to analyse the local front shearing governed by poloidal flows with large poloidal mode numbers. The underlying difference with the zonal flow stabilisation criterion is the fact that the SOL appears to be dominated by localised bursts of transport events. The properties of test-particle transport are used to revisit the intermittent property that is usually pinned to the SOL

turbulence. It is shown that the SOL turbulence is weakly intermittent in the neutral fluid terminology. Rather, it appears to be governed by relaxation events that trigger the bursts of turbulent transport. This shift in understanding is a powerful tool to explain the universal results of SOL turbulence that cover a large variety of magnetic configurations including linear devices that do not exhibit any significant interchange drive. It also offers a natural bridge to the ELMs relaxation events. Last and not least, it is shown that the density structures exchange rapidly particles with the neighbouring plasma since test particles exhibit velocities that are much larger than the density structure itself. This mixing effect is a drive towards thermodynamical equilibrium of the density structure with the SOL background. Section 3 is dedicated to the interaction between open and closed field lines based on a 2D (radial and parallel) transport code with ad-hoc diffusive radial transport for momentum and density [6]. The results are focussed on the velocity imprint from the SOL plasma into the core plasma and its dependence on the magnitude of the diffusive transport of parallel momentum. Finally, the results of the TOKAM-3D code [7], a full torus edge and SOL turbulence and transport code, are presented in Section 4. This simulation work allows one to recover quantitatively the parallel Mach number ($M_{//}$) flow pattern reported in the experiments and in particular on Tore Supra [2].

2. Turbulent Front Propagation and Shearing in the SOL

We restrict the analysis to the density at constant temperature in the cold ion limit. In the TOKAM-2D model, the system is governed by two equations, one for the normalised density field N and the other for the normalised electric potential ϕ. The flute assumption allows one to reduce the space to x and y respectively the radial and poloidal coordinates. These are normalised to the hybrid Larmor radius ρ_s, $\rho_s^2 = T_e / m_i$ (T_e is the electron temperature and m_i is the ion mass ratio), time to the ion cyclotron frequency Ω_i. Although very simplified, this system, when flux driven, appears to be generic of SOL transport [5].

$$\left(\partial_t + \{\phi\} - D\nabla_\perp^2\right) Log(N) - D(\nabla_\perp Log(N))^2 = -\sigma e^{(\Lambda-\phi)} + S/N \qquad (1a)$$

$$\left(\partial_t + \{\phi\} - \nu\nabla_\perp^2\right)\nabla_\perp^2\phi + g\partial_y Log(N) = \sigma\left(1 - e^{(\Lambda-\phi)}\right) \qquad (1b)$$

In this system the bracket term $\{\phi\}f$ stands for the Poisson bracket between ϕ and f, and represents the $E\times B$ convection. In this set of equation, we have made full use of the fact that the Vlasov equation in homogeneous with respect to the distribution function (the distribution function can be multiplied by any constant with no change of the equation). Accordingly, most of the terms in Eq. (1) depend on $Log(N)$. Consequently, the suitable representation of the density field is $Log(N)$ whenever collisions or specific source terms are not dominant. This property leads us to reconsider the strongly skewed density PDFs previously published [5] to much more Gaussian PDFs when $Log(N)$ is considered. In particular, the PDFs of the two active fields, namely $Log(N)$ and ϕ, are then comparable, Fig. 1. In that framework, edge plasma turbulence appears to be less specific when compared to neutral fluid turbulence. A more in depth comparison between neutral fluid turbulence and SOL turbulence is addressed in [Morize]. It appears that edge plasma turbulence differs from homogeneous neutral fluid turbulence due to the occurrence of relaxation processes that are characteristic of these flux driven systems. Each relaxation process generates over-dense and sub-dense structures coupled to electrostatic dipoles that propagate ballistically in the SOL. We refer to these bursts of turbulence as fronts.

Of interest for the transport properties of these fronts is the exchange with the SOL background. Indeed, it can be noticed that the $E\times B$ velocity within the front of the order of

$0.06\,c_s$ is a about a factor 2 larger than that of the front motion. The calculation with test particles exemplifies the relative motion of the front and the test particles. The particles are initiated randomly within the density structure and then move according to the Hamiltonian dynamics leading to the $E\times B$ velocity. Particles rapidly catch-up the forefront and then are ejected poloidally. The typical life time of the test particles within the overdense front is $\Omega_i\tau_{life}\approx 10^3$ thus comparable to the time required to cover the extent of the front $\approx 30\rho_s$ at the relative velocity $\approx 0.03c_s$. This property is important to analyse the transport properties of these fronts. Indeed, the rapid test particle mixing on times shorter than the front lifetime leads to some thermodynamical equilibrium between the front and the SOL background, The content of the front in the far SOL will thus differ from the content of the front where it is generated, thus reducing the impact of these events on impurity transport or prompt energy deposition via the front propagation from the separatrix to the chamber wall. Shearing by local poloidal flows strongly enhances this mixing property since these flows induce elliptic points with positive exponentiation factors in the Hamiltonian $E\times B$ motion, as addressed in the following.

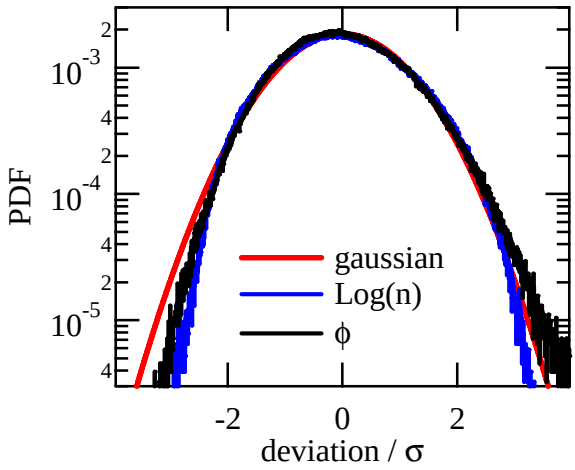

FIG 1: Probability Distribution Function of the density $Log(N)$, blue curve, and electric potential ϕ, black curve versus the deviation normalised by the standard deviation σ. The red curve is the Gaussian computed with the normalised deviation.

Following the Rapid Distortion Theory [pope], let us decouple the evolution of the density front from that of the electric potential and impose Λ as two superimposed structures, $\Lambda_s(y)=-\phi_s\sin(ky)$ and $\Lambda_z(x)=\phi_z\exp\left(-(x-x_z)^2/(2\Delta_z^2)\right)$. In this approach, the motion of the structure is fully governed by the $E\times B$ drift. The s subscript refers to streamer while the z subscript refers to zonal although the imposed electric potential does not originate from those basic mechanisms. Minimising the parallel current outflow in Eq. (1b) ensures that $<\phi>=\Lambda_s+\Lambda_z$. The Poisson bracket term in Eq. (1a) then governs the convection of the density field. It combines therefore the radial convection by $\Lambda_s(y)$ with wave vector k and a velocity shear layer with poloidal convection localised at $x=x_z$ with an extent Δ_z: $\dot{x}=V_{Ex}$, $\dot{y}=V_{Ey}$ hence $\dot{x}=-\partial_y\phi=-\partial_y\Lambda_s$ and $\dot{y}=\partial_x\phi=\partial_x\Lambda_z$. In the region $|x-x_z|>>\Delta_z$, the motion of the density structure is governed by the radial velocity $V_{Ex}=k\phi_s\cos(ky)$, $V_{Ex}\approx k\phi_s$ when $ky<<1$. Let us consider a circular density structure such that $t=0$, $x_0^2+y_0^2=\Delta_0^2$ with $k\Delta_0<<1$. This structure will drift towards the shear layer at constant velocity and without changing shape. Upon reaching the shear layer the density structure will be distorted, but this effect will take

place at constant electric potential determined by the initial condition. Indeed, according to the Hamiltonian equations of motion, the potential ϕ is conserved as well as the surface of the density structure. Provided $|ky| < \pi/2$, one then obtains: $y = y_0 + \Delta y \cdot \exp\left(-(x-x_z)^2/(2\Delta_z^2)\right)$ with $\Delta y = \phi_z/(k\phi_s)$ and $x = x_0 + (k\phi_s)t$ together with $\left(x-(k\phi_s)t\right)^2 + \left(y - \Delta y \cdot \exp\left(-(x-x_z)^2/(2\Delta_z^2)\right)\right)^2 = \Delta_0^2$. The conservation property then ensures that if $\phi_z \geq \phi_s$, no elliptic point is formed in the equipotentials and the shear layer cannot be crossed thus leading to a strong transport barrier. Let us consider the stopping capability of a shear layer in the case of a weaker transport barrier. The effect of the shear layer is analysed in the case of a circular density structure initialised in a linear shear layer with constant poloidal velocity V_z, and constant velocity shearing rate $1/\tau_z = dV_z/dx$. With these assumptions one obtains the time dependent shape of the density structure $x^2 + \left(y - V_z t - xt/\tau_z\right)^2 = \Delta_0^2$. Defining the poloidal extent of the structure Δ_y as half the distance between the two points with derivative $dy/dx = 0$, one obtains $\left(\Delta_y/\Delta_0\right)^2 = 1 + \left(t/\tau_z\right)^2$ that allows one to estimate the half radial extent from the surface conservation taken as $\Delta_x \Delta_y = \Delta_0^2$. Thus, as the poloidal extent of the density structure is increased, the radial gradient, $\approx \delta n/\Delta_x$, where δn is the magnitude of the density front, is also increased. These geometrical properties will therefore boost the diffusion process so that the net particle outflux, of the order of $D\delta n L_{//}\Delta_y/\Delta_x$ where $L_{//}$ is the parallel elongation of the front, will govern the decrease of the number of particles within the density contour $\partial_t\left(\delta n L_{//}\Delta_0^2\right)$. Combining these expressions, one finds that the density within the contour will decay exponentially, $\delta n(t) = \delta n_0 \exp\left(-t/\tau_d - t^3/(3\tau_D^3)\right)$, where the diffusive time scale is $\tau_d = \Delta_0^2/D$ and τ_D, the Dupree time is $\tau_D = \left(\tau_d \tau_z^2\right)^{1/3}$. The thinning of the structure by the shearing effects governs the enhanced diffusive outflux and leads to the Dupree time. Given the values of the parameters chosen for the simulations, one finds $\tau_D/\tau_d \approx 1/20$. In the turbulent self-organised case with shear layers generated in the wake of prior fronts, one finds that the poloidal and radial Mach numbers are comparable, typically in the range of 0.03 and , the Dupree time of the order of $\tau_D \Omega_i \approx 1500$, so that one finds that the poloidal distance covered by the density structure before its collapse is $L_D = \tau_D M_\theta$, $L_D \approx 45\rho_s$,given the typical turbulence wave length $k_\theta \rho_s \approx 0.3$, one finds that the required wave vector required for effective shearing is $K_\theta \rho_s \approx 0.06$.

3. 2D Diffusive Spreading of SOL and Edge Flows

A 2D transport model is used to investigate the issue of flow spreading between the open and closed field lines. The limiter particle loss, with the standard Bohm boundary conditions, balances a source of particles due to a prescribed particle influx at the core boundary. Cross-field transport is assumed to be homogeneous diffusion with particle diffusion coefficient $D_\perp$ and momentum diffusion $\nu_\perp$. The considered 2D geometry is the (r,s) plane where s is the curvilinear abscissa along the magnetic field. The core region is assumed periodic in s with $L_{//}$ the total length. The SOL region has a similar parallel scale (the limiter has a vanishing extent along s). This 2D model allows one to address the issue of flow spreading as well as to investigate the discontinuities at the edge/SOL interface, for instance the occurrence of Kelvin-Helmholtz instabilities at the limiter head. Assuming constant temperature as in the previous model, the two fields that are considered here are thus

the density n and the parallel Mach number $M_{//}$. The two coupled equations depend on the sound velocity $c_s^2 = (T_e + T_i)/m_i$ and have the form of the density and momentum balance equations.

$$\partial_t n + M_{//} c_s \partial_s n - \partial_r (D_\perp \partial_r n) + n c_s \partial_s M_{//} = 0 \qquad (2a)$$

$$\partial_t (n M_{//}) + M_{//} c_s \partial_s (n M_{//}) - \partial_r (\nu_\perp \partial_r (n M_{//})) + n M_{//} c_s \partial_s M_{//} + c_s \partial_s n = 0 \qquad (2b)$$

For steady state conditions and with $\nu_\perp = 0$, the second equation takes the form $\partial_s \Pi = 0$, where Π is the total pressure $\Pi = n(T_e + T_i)(1 + M_{//}^2)$. Departure from the parallel conservation of Π in steady state solutions is therefore a consequence of the transverse momentum transport governed by $\nu_\perp$. In this analysis, we focus our attention on the spreading properties of the flows, keeping as much as possible the density field constant. To that purpose we normalise time to $\tau_{//} = L_{//}/c_s$, parallel scales to $L_{//}$ and transverse scales to the particle diffusive scale $\lambda^2 = D\tau_{//}$. The parallel flow velocity is implicitly normalised to c_s yielding $M_{//}$. As in Section 2, the system is homogeneous with respect to n and $Log(n)$ would have been a more appropriate normalised field. The normalised equations in slab geometry with $t = \tau_{//}\tau$, $s = L_{//} z$ and $r = \lambda x$ are then:

$$\partial_\tau n + M_{//} \partial_z n - \partial_x^2 n + n \partial_z M_{//} = 0 \qquad (2a)$$

$$\partial_\tau (n M_{//}) + M_{//} \partial_z (n M_{//}) - S_c \partial_x^2 (n M_{//})) + n M_{//} \partial_z M_{//} + \partial_z n = 0 \qquad (2b)$$

This equation only depends on one control parameter, namely the Schmidt number $S_c = \nu_\perp / D_\perp$. The other control parameters are related to the geometry, namely the aspect ratio $A = \delta_{SOL}/L_{//}$, the normalised SOL width $\Delta_{SOL} = \delta_{SOL}/\lambda$, the normalised edge width $\Delta_{edge} = \delta_{edge}/\lambda$ and those related to the boundary conditions, the Mach number at the limiter, formally set by the Bohm boundary conditions, $M_{//}^2 = 1$, the Mach number at the core edge boundary M_{core} as well as the particle influx from the core, $\Gamma_{core} = \partial_x n\big|_{core}$. At the wall boundary less relevant conditions are applied, $\partial_x n\big|_{wall} = 0$ and $\partial_x (n M_{//})\big|_{wall} = 0$. In the limit $\Delta_{SOL} >> 1$, and $A >> 1$ these boundary conditions have little impact on the solution. Furthermore, the magnitude of the density is determined by the core influx and the space dependence of the steady state solution is therefore prescribed but for the effect of the coupling to the Mach number through the term $\partial_z (n M_{//})$. The coupling of the edge plasma parallel convection to the SOL parallel convection is readily observed, see Fig. 2. The maximum of the Mach number induced in the edge plasma decays radially. Furthermore, when considering the parallel dependence, one finds an increase from the stagnation point $z = 0$ where $M_{//} = 0$ to a maximum $(z_{\max}, M_{\max})$ value and then decays back to $M_{//} = 0$ at $z = 1$. The decay of the value $M_{\max}$ as the radius is reduced from the limiter radius $x = 0$ towards the core $x = -5$ is very sharp in the vicinity of the last closed flux surface and then more gradual. One can also observe that the parallel position of the maximum, $z_{\max}$, is shifted away from the limiter position as the radius is decreased. The complex behaviour associated to the diffusion of the plasma momentum from the SOL to the core plasma is still under investigation. It also appears that in the present simulations, the variation of the Schmidt number S_c does not strongly modify either the density field or the parallel velocity field.

Conversely, imposing a given flow at the core boundary, $M_{core} = 0.3$ governs a strong asymmetry of the SOL, and, similarly to the Mach probe theory, a density imbalance between both sides of the limiter. Such an imbalance will also drive an imbalance in the energy flux to the limiter, a feature that routinely is reported in the experiments.

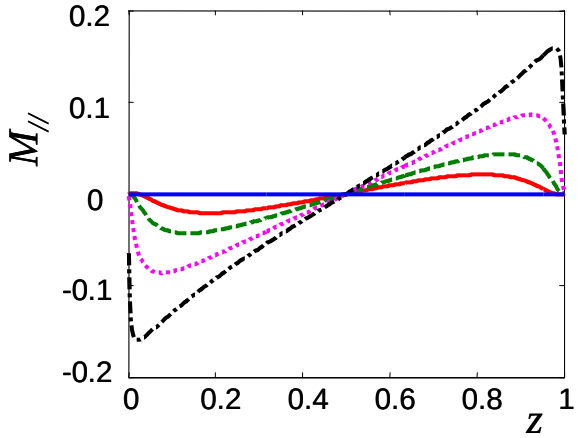

FIG. 2: Parallel profiles of velocity for $\Delta_{SOL} = 5$, $S_c = 1$ at different radii within the edge, $x = -5$ (blue), $x = -4$ (red), $x = -3$ (green), $x = -2$ (pink), $x = -1$ (black).

4. SOL and Edge Flow in Full Torus Simulations with the Code TOKAM-3D

The TOKAM-3D model discussed here is based on the equations for the density, the parallel Mach number and the vorticity at constant electron and ion temperature. The magnetic geometry is cylindrical but with varying magnitude of the magnetic field as in a torus. The normalised equations are then

$$LN + BN\nabla_{//}\left(\frac{M_{//}}{B}\right) - B\nabla_{//}\left(\frac{J_{//}}{B}\right) + BT_e\left\{\frac{1}{B^2}\right\}N - BN\left\{\frac{1}{B^2}\right\}\phi = S_N \qquad (3a)$$

$$LM_{//} + \frac{T_e + T_i}{N}\nabla_{//}N = S_M - \frac{M_{//}}{N}S_N \qquad (3b)$$

$$LW - \frac{B^3}{N}\nabla_{//}\left(\frac{J_{//}}{B}\right) + \frac{B^3(T_e + T_i)}{N}\left\{\frac{1}{B^2}\right\}N = 0 \qquad (3c)$$

$$L = \partial_t + M_{//}\nabla_{//} + \{\phi\} - D_\perp\nabla_\perp^2 \quad ; \quad W = \nabla_\perp^2\phi + \frac{T_i}{N}\nabla_\perp^2 N \quad ; \quad \eta N J_{//} = T_e\nabla_{//}N - N\nabla_{//}\phi$$

For the sake of simplicity the same linear operator L is introduced although in practice different diffusion operators can be considered hence leading to different operators L. As in the previous section one considers here constant ion and electron temperature. Within respect to the previous systems the new important terms are related to the magnetic field curvature, encountered for by the Poisson bracket operator $\{1/B^2\}$ and to the electric current. Similar boundary conditions to the previous sections are used and buffer regions with enhanced diffusion are introduced at the boundaries to suppress the turbulent fluctuations at the boundaries. As in Section 2, the simulation domain is an edge annulus, typically from $r/a = 0.5$ to $r/a = 1.5$, hence comprising the edge and SOL plasma, in full torus. The code can be operated in the turbulent regime with small $D_\perp$ as well as in transport regime with large ad-hoc $D_\perp$. The code is first run with large ad-hoc diffusion terms. In such a regime, all instabilities are damped and axisymmetric equilibriums are reached with the appropriate large

scale flows and currents. We refer to these regimes as neo-classical transport regimes. Let us consider such a neoclassical regime with $D_\perp = 0.2$, the location of the limiter being at the bottom, $\theta = 0$, with ion ∇B drift oriented downwards. In such a regime, one recovers the characteristic parallel Mach number poloidal variation as reported experimentally [2], Fig. 3.

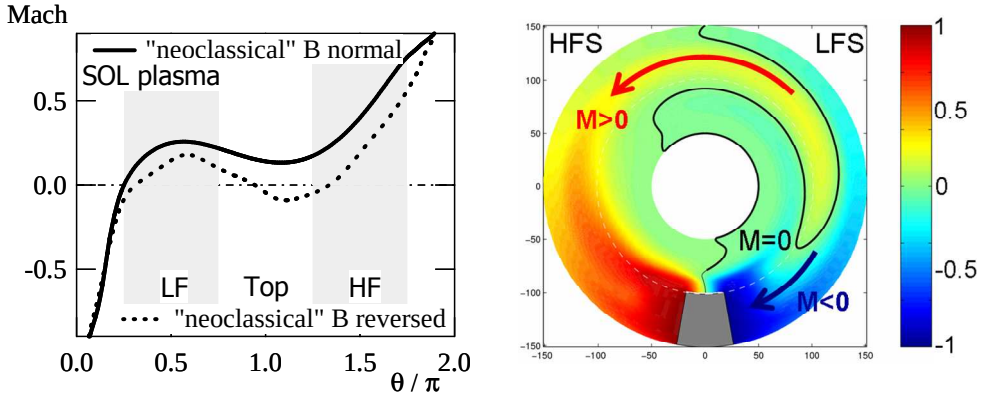

FIG. 3: poloidal cut of the parallel Mach number with diffusive transport, right hand side, and poloidal variation in the SOL at r/a = 1.07, left hand side.

At the top of the device ($\theta = \pi$), the large values of $M_{//}$ are located in the SOL with a maximum reaching $M_{//} = 0.2$. The occurrence of such flows is not therefore completely related to poloidally asymmetric radial fluxes of particles. It is interesting to notice that reversing the magnetic field, hence with ion ∇B drift towards the top, has a weak effect on the flow pattern although the flow magnitude at the top is reduced, Fig. 3. The reversal of the magnetic field also governs the reversal of radial gradient of the mean electric potential throughout the system. Such a behaviour is consistent with the basic symmetry of most of the terms in Eq. (3a, 3b, 3c), namely that the magnetic field reversal, leading to a change in sign of the Poisson brackets that can be compensated by changing the sign of the electric potential variations, thus leaving most of the terms unchanged, but for the curvature operator applied to N. The latter term governs a radial particle flux towards or away from the top region that could be large enough to generate the observed differences.

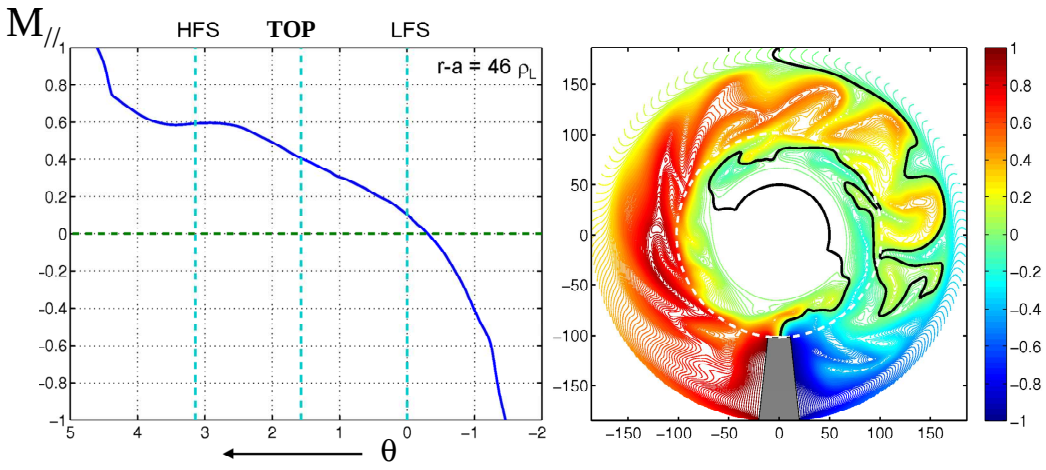

FIG. 4: poloidal cut of the parallel Mach number in the turbulent regime, right hand side, and poloidal variation in the SOL, left hand side.

The poloidal $E \times B$ flow from the high field side to the low field side can be estimated following the calculation of the GAM frequency taking into account the resistive and diffusive damping. However, non-linear calculations are required to obtain the effect on the

particle parallel flux variation, since the $E \times B$ flow is large enough to balance the parallel flow, and can therefore also convect poloidally the parallel Mach number. Although the neoclassical regime allows one to recover qualitatively the experimental results on the poloidal variation of the Mach number, the quantitative agreement is only reached in the turbulent regime, Fig. 4. The ballooning nature of turbulent transport then enhances the parallel flow and $M_{//} = 0.4$ is reached near the top. The simulation of the edge plasma coupled to the SOL indicates that turbulence triggers ballistic transport events deep into the SOL plasma that spread the previously described parallel Mach number pattern from the edge into the SOL. These results are in agreement with the Tore Supra experiments [2] and the data base of edge flows in X-point devices [3, 4].

5. Discussion and Conclusion

The complex turbulence and large scale flow in the edge and SOL plasma is addressed with 3 different simulation codes. SOL turbulence properties are investigated with the TOKAM-2D code. It is found that the departure between the SOL plasma turbulence and the neutral fluid turbulence regarding intermittency is far less pronounced when $Log(N)$ is considered rather than N. Furthermore, the density fronts are observed to exhibit rapid mixing with the background SOL and to be sensitive to shearing effects for finite wave length poloidal flows. Regarding the latter, and more broadly the large scale flows that build-up in the SOL and edge steady state, a 2D diffusive transport code shows that flow spreading does occur between the SOL and the edge plasma but that this effect is restricted to a very narrow region in the vicinity of the separatrix and weakly dependent on the control parameter. Finally the 3D full torus code TOKAM-3D is used to investigate transport end turbulence properties. In the diffusive transport regime, also called neoclassical, one finds that the radial electric field plays a strong role in the flow pattern, both by counteracting the parallel flow and by convecting this flow poloidally. The bottom line is that the stagnation point of the parallel flow is shifted to the low field side and Mach 0.2 parallel flow builds-up at the top of the device from the low field side to the high field side as reported experimentally. In the turbulent regime this effect is enhanced by the ballooned turbulent outflux so that the Mach number at the top of the device reaches Mach 0.4 in qualitative agreement with experimental evidence. The facts collected by this analysis are consistent with the picture of SOL turbulence generated by relaxation events –the latter governing some intermittency but comparable to that of neutral fluids- where the SOL parallel flows and cross-field transport appear to have little impact on the edge transport, while the edge conditions and in particular the large scale flows modify the SOL properties.

Acknowledgements

Part of this work was carried out in the framework of the ANR project M2TFP. The authors have also benefited from the discussions held during the Festival de Théorie held in Aix en Provence.

References

[1] Progress in the ITER physics basis, Nucl. Fusion, 47 (2007)
[2] J. Gunn et al., J. Nucl. Mater., **363-365** (2007) 484
[3] R. Pitts et al., J. Nucl. Mater., **337–339** (2005) 146
[4] N. Asakura et al., J. Nucl. Mater., **363-365** (2007) 41
[5] Y. Sarazin et al. Phys. Plasmas, **5** (1998) 4214
[6] G. Ciraolo et al., to be published in J. Nucl. Mater.
[7] P. Tamain et al., to be published in J. Nucl. Mater.